JOURNAL OF ENDOUROLOGY
Volume 26, Number 2, February 2012

Pp. 183–189
DOI: 10.1089/end.2011.0349

Endoscopic Assessment and Prediction of Prostate Urethral Disintegration After Histotripsy Treatment in a Canine Model*

George R. Schade, M.D.,[1] Nicholas R. Styn, M.D.,[1] Timothy L. Hall, Ph.D.,[1,2] and William W. Roberts, M.D.[1,2]

Abstract

Background and Purpose: Histotripsy is a nonthermal focused ultrasound technology that uses acoustic cavitation to homogenize tissue. Previous research has demonstrated that the prostatic urethra is more resistant to histotripsy effects than prostate parenchyma, a finding that may complicate the creation of transurethral resection of the prostate-like treatment cavities. The purpose of this study was to characterize the endoscopic appearance of the prostatic urethra during and after histotripsy treatment and to identify features that are predictive of urethral disintegration.

Materials and Methods: Thirty-five histotripsy treatments were delivered in a transverse plane traversing the prostatic urethra in 17 canine subjects (1–3/prostate ≥ 1 cm apart). Real-time endoscopy was performed in the first four subjects to characterize development of acute urethral treatment effect (UTE). Serial postprocedure endoscopy was performed in all subjects to assess subsequent evolution of UTE.

Results: Endoscopy during histotripsy was feasible with observation of intraurethral cavitation, allowing characterization of the real-time progression of UTE from normal to frank urethral disintegration. While acute urethral fragmentation occurred in 3/35 (8.6%) treatments, frank urethral disintegration developed in 24/35 (68.5%) within 14 days of treatment. Treating until the appearance of hemostatic pale gray shaggy urothelium was the best predictor of achieving urethral fragmentation within 14 days of treatment with positive and negative predictive values of 0.91 and 0.89, respectively.

Conclusion: Endoscopic assessment of the urethra may be a useful adjunct to prostatic histotripsy to help guide therapy to ensure urethral disintegration, allowing drainage of the homogenized adenoma and effective tissue debulking.

Introduction

Surgical therapy for benign prostatic hyperplasia (BPH) has consisted of endoscopic debulking of the prostate for decades, with transurethral resection of the prostate (TURP) being considered the gold standard. More recently, laser-based therapies, including photovaporization of the prostate and holmium laser enucleation of the prostate, have emerged as promising alternative debulking therapies with decreased morbidity compared with TURP.[1,2] These therapies, however, remain invasive with associated surgical risks. As a result, less invasive technologies have been pursued, including transurethral microwave thermotherapy and transurethral needle ablation, which thermally coagulate BPH tissue while sparing the urethra from damage.[3] While these approaches achieve therapeutic benefit, they have failed to replicate the efficacy and durability of TURP.[4,5] These deficiencies combined with many men now presenting later in life with greater comorbidities and greater risk of preoperative complications and morbidity[6] have created a need for the development of less invasive treatment modalities that replicate the tissue debulking achieved with TURP.

Histotripsy, an experimental noninvasive extracorporeal focused ultrasound (US) technology, is capable of fractionating prostate tissue in an *in vivo* canine model with resultant tissue debulking.[7] Histotripsy involves delivery of high amplitude, short (4 μs) pulses of US energy to a cigar-shaped geometric focal volume resulting in the development of microbubbles. The oscillation, coalescence, and collapse of these bubbles produces mechanical fractionation of targeted tissues, reducing tissue architecture and cellular structures to a fine slurry of acellular debris. Volumetric ablation is accomplished by moving the transducer focal volume throughout the targeted region. As the tissue is converted to homogenate, the US appearance becomes progressively hypoechoic.[8–11] Transabdominal histotripsy of the prostate is safe and

Departments of [1]Urology and [2]Biomedical Engineering, University of Michigan, Ann Arbor, Michigan.
*Videos demonstrating the technique are available at www.liebertonline.com/end

effective in an *in vivo* canine BPH model,[12] producing dose-dependent tissue debulking of the adenomatous BPH tissue[13] with minimal hematuria, even in an anticoagulated model.[14]

The strategy for the development of histotripsy therapy for BPH is to produce a TURP-like defect. To achieve this goal, the prostatic urethra as well as the adjacent parenchymal tissue must be fractionated. Previous work has demonstrated the prostatic urethra to be more resilient to histotripsy than prostate parenchyma, necessitating a greater number of acoustic pulses to achieve tissue disintegration.[13] In addition, unlike the progressive US changes seen with parenchymal homogenization, prostatic urethral disintegration is difficult to discern with real-time US imaging.

In this study, we sought to endoscopically visualize and characterize the chronology of prostatic urethral tissue changes induced by histotripsy. Furthermore, we hypothesized that characteristic endoscopic tissue features resulting from histotripsy would be predictive of subsequent urethral disintegration.

Materials and Methods

Subjects

After receiving approval from the university committee for animal use and care, 18 intact male canine subjects weighing 25.0 to 33.6 kg were obtained. Subjects were anesthetized with subcutaneous acepromazine (0.1 mg/kg) and intravenous propofol (2-8 mg/kg) and intubated. They were prepped with a tap water enema with digital rectal disimpaction after intubation. The lower abdomen and suprapubic region were shaved before positioning each subject supine on the procedural table. Inhalational anesthesia (isoflurane 1%–2%) was maintained throughout treatment. All subjects received intramuscular penicillin G benzathine (40,000 IU/kg) before the procedure and on postoperative (POD) days 3 and 7 for prophylaxis. Carprofen (2.2 mg/kg/d) was administered orally before the procedure and for 24 hours afterward for analgesia. Flexible endoscopy was performed with an 8.2F flexible ureteroscope (DUR-8, Gyrus ACMI, Southborough, MA) before histotripsy treatment to document a normal lower urinary tract and to serve as an intrasubject control. No urinary catheter was left in place after treatment.

Experimental setup and procedure

Transrectal US (TRUS) imaging was performed using a Logiq 6 US scanner (GE Healthcare, Waukesha, WI) with a model ERB probe positioned manually and fixed in a custom holder. The prostate volume was estimated using the stepper volume technique tracing the prostate perimeter on transverse slices at 2.5 mm intervals. The therapeutic system consisted of a 16-element piezoceramic composite array (750 kHz, 11×14-cm diameter oval shape, focal length 10 cm, focal volume 3×3×8 mm; Imasonic, Voray sur l'Ognon, France) on a three-axis computer-controlled positioning system (MATLAB, MathWorks, Natick, MA). Coupling was achieved by placing the therapy transducer in a bath of degassed water contained in a plastic membrane in direct contact with the shaved abdomen.

One subject received sham treatment, and 17 subjects received histotripsy treatment. Histotripsy pulses consisted of five cycle bursts of acoustic energy at 750 kHz, with a duty cycle less than 1% and pulse repetition frequency ranging from 50 to 2000 Hz. Each treatment consisted of delivery of 3000 to 100,000 histotripsy pulses per mm of the treatment path on a single transverse plane that intersected the urethra and periurethral tissues (Fig. 1). A total of one to three treatments separated by at least 1 cm along the apex-base axis were delivered per prostate, dependent on prostate length.

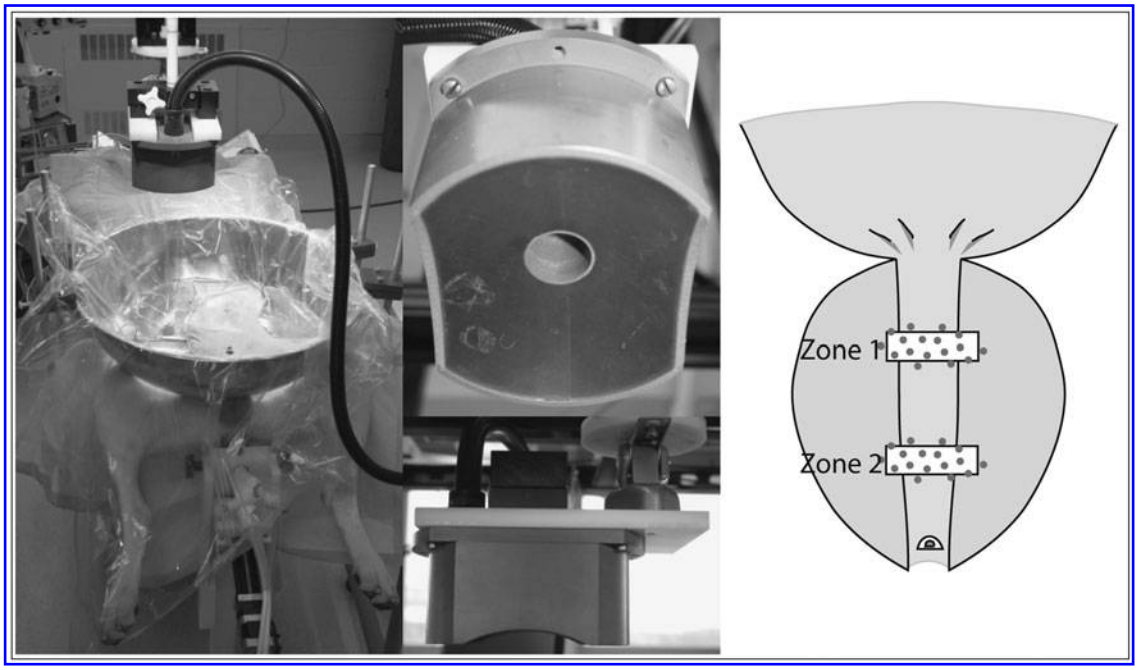

FIG. 1. Experimental setup with coupling bath of degassed water positioned over suprapubic region of supine canine subject. The histotripsy transducer is suspended in the water bath and translated to create transverse treatment planes transecting the prostatic urethra.

Histotripsy treatment was performed in the first four subjects with the flexible ureteroscope positioned in a retrograde fashion just distal to the treatment zone on TRUS to minimize effect on treatment, yet allow intraurethral visualization of the cavitation cloud.

Postprocedure care and endoscopic evaluation

After completion of histotripsy treatment, cystoscopy was performed to evaluate for acute changes in urethral appearance. All subjects recovered from anesthesia and were monitored for treatment-related adverse events. Cystoscopy was repeated on PODs 1, 3, 7, and then weekly until euthanasia. Repeated TRUS under anesthesia was repeated weekly until euthanasia. Ten subjects were euthanized on POD14 as initially planned. Two subjects were euthanized early on POD 2 after development of intraperitoneal urinoma secondary to full thickness prostatic urethra and parenchymal disintegration through the capsule. Four subjects with normal endoscopy despite TRUS evidence of homogenization of parenchymal tissue adjacent to the prostatic urethra were maintained to POD 21 to allow further chronologic assessment of the urethra. Two subjects in which urethral disintegration developed before POD 14 were maintained to POD 28 to assess the evolution of the treatment cavity.

At the time of euthanasia, TRUS imaging and retrograde endoscopy (with flexible ureteroscope) were performed. Next, a suprapubic incision was made and a cystotomy created through which antegrade cystourethroscopy was performed using a 16F flexible cystoscope (Cy2, Olympus). The prostate, bladder, and adjacent rectum were then surgically removed *en bloc*. The prostate, bladder, and rectal tissues were inspected grossly for injury. Harvested prostates were fixed in formalin for 1 week, cut into 5-mm thick slabs, dehydrated in 25% ethanol, paraffin embedded, cut using a microtome in 5-μm sections at 1-mm increments, mounted, and stained with hematoxylin and eosin for histologic assessment.

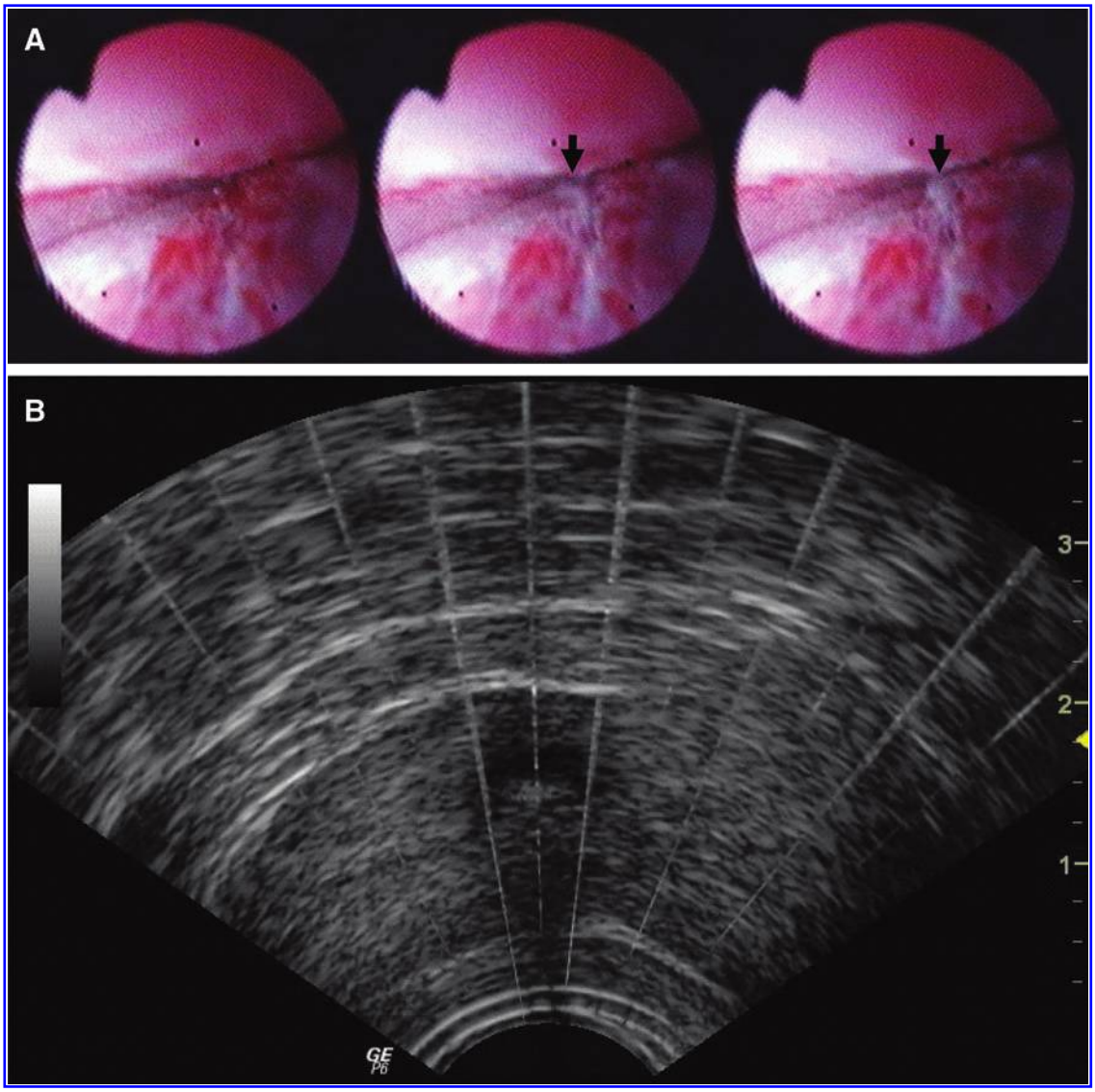

FIG. 2. Endoscopic appearance of urethra at $\sim$0.5 s intervals with bubble cloud (at tip of arrow) in urethral lumen **(A).** Transrectal ultrasound appearance of histotripsy bubble cloud in urethral wall and lumen during treatment **(B).**

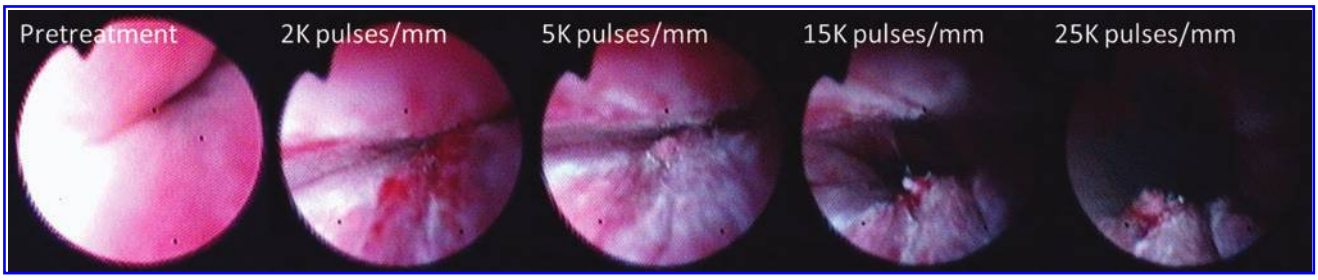

FIG. 3. Real-time endoscopic surveillance of histotripsy treatment showing normal pretreatment urethra and prostate histotripsy treatment effect at 2000, 5000, 15,000, and 25,000 pulses/mm of treatment path in the same subject. Note the development of petechial hemorrhage (2000 pulses/mm) followed by hemostasis and the appearance of shaggy gray urothelium (5000 pulses/mm) and subsequently a small flap of tissue (15,000 pulses/mm). (The urethra has rotated slightly from pretreatment to treatment secondary to compression from extracorporeal water.)

Statistical analysis

The reliability of postprocedure endoscopic findings on POD–0 to predict the development of macroscopic urethral fragmentation/disintegration was evaluated using sensitivity, specificity, and positive (PPV) and negative (NPV) predictive value.

Results

A total of 35 prostate histotripsy treatments (1-3 treatments per prostate, dependent on prostate size) were applied to 17 canine subjects, and a sham procedure was performed on 1 subject. Mean prostate volume was 20.7 ± 5.2 cc. During the course of histotripsy treatment, the cavitation bubble cloud was easily seen with TRUS, and targeted parenchymal tissue became progressively hypoechoic while the urethra appeared structurally intact on US images.

Flexible endoscopy performed during histotripsy therapy in the first four subjects (six treatments) provided direct intraluminal visualization of the cavitation bubble cloud as it traversed the urethral lumen (Fig. 2) (supplementary videos demonstrating the technique are available at www.liebertonline.com.end) and revealed a dose-dependent progression of treatment effect. Visualized urethral treatment effect began with as few as 2000 to 3000 pulses/mm of treatment path, producing petechial hemorrhage and active bleeding (Fig. 3). These findings evolved to relative hemostasis and the appearance of pale, shaggy, shedding urothelium with further treatment in as little as 5000 to 10,000 pulses/mm in the most susceptible subject. With continued treatment, small flaps of urethral tissue formed that coalesced before frank urethral disintegration.

Endoscopy immediately after histotripsy (POD 0) revealed normal appearing urethra between targeted transverse treatment planes in subjects undergoing more than one treatment per prostate, demonstrating tight confinement of treatment effect. While gross urethral disintegration was apparent in 3/35 (8.6%) treatment zones on POD 0 endoscopy, it developed in 24/35 (68.5%) by POD 14. POD 0 and subsequent endoscopic appearance of the prostatic urethra did not differ between the four subjects undergoing endoscopy during active treatment and those that did not. In subjects maintained to POD 21, no additional urethral disintegration was observed after POD 14.

Transverse treatment planes without endoscopically observed urethral disintegration by POD 14 were found on TRUS to have persistent internal echoes and/or a gravity fluid/debris line within the adjacent targeted parenchyma, while planes with cavities communicating with the urethra had absent or minimal internal echoes consistent with drainage of the homogenized material via the urethra. These findings were confirmed histologically (Fig. 4). The sham subject's urethra

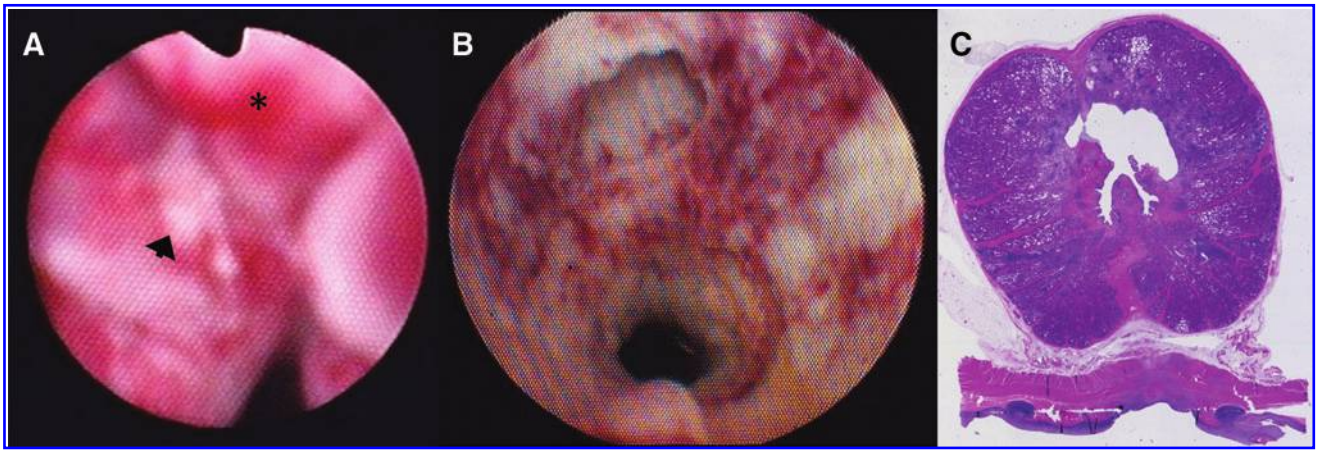

FIG. 4. Endoscopic appearance of the prostatic urethra immediately after histotripsy treatment, demonstrating grade 1 (*) and grade 2 (arrowhead) treatment effect **(A),** and on postoperative day 14 demonstrating urethral disintegration **(B),** with confirmatory histologic findings **(C)** in the same subject.

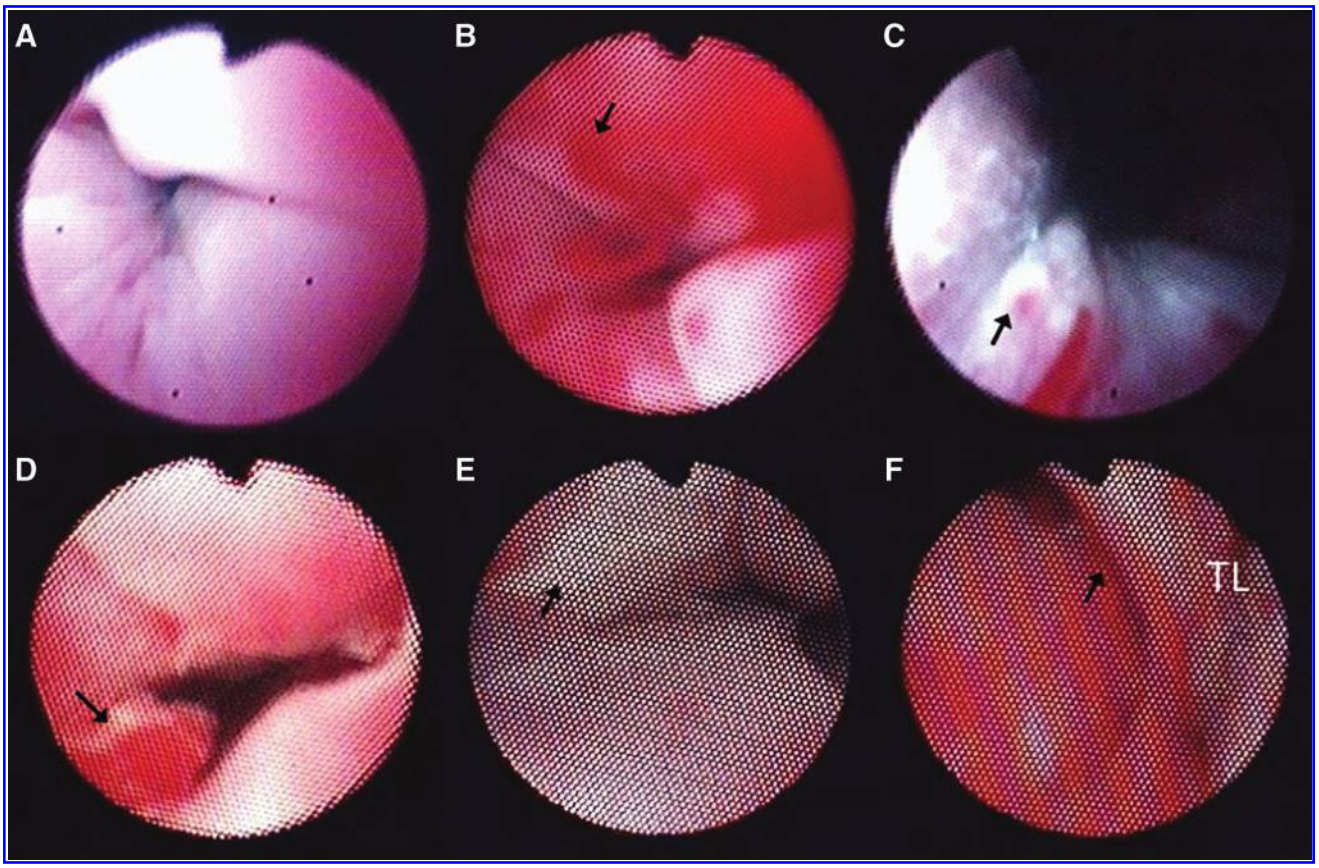

FIG. 5. Endoscopic grading scale of prostatic urethral histotripsy treatment effect. **(A)** Appearance of normal untreated urethra. **(B)** Appearance of grade 1 damage (active bleeding ± petechial hemorrhage), **(C)** grade 2 damage (shedding urothelium), **(D)** grade 3 damage (urothelial flap), **(E)** grade 4 damage (urethral wall necrosis), **(F)** grade 5 (frank urethral disintegration/perforation). TL = true lumen.

and prostate remained normal throughout the postprocedure period on serial endoscopy and TRUS, respectively.

Using the real-time endoscopy data, a grading scale (0 = normal, 1 = active bleeding and/or petechial hemorrhage, 2 = urothelial shedding, 3 = urothelial flap, 4 = urethral wall necrosis, 5 = frank urethral disintegration/perforation) was constructed (Fig. 5) to characterize the endoscopically apparent degree of urethral treatment effect. Immediate POD 0 endoscopy was interpretable in all cases except for two subjects (accounting for four treatment zones) in which equipment damage prevented adequate visualization; these subjects were excluded from the analysis. Of the 31 endoscopically evaluable treatment planes, POD 0 endoscopy revealed ≥ grade 1 treatment effect in 28/31, ≥ grade 2 effect in 22/31, and ≥ grade 3 effect in 9/31. Presence of at least grade 1 treatment effect had PPV and NPV of 0.75 and 1.00, respectively, for subsequent development of urethral disintegration by POD 14 (Table 1). Presence of at least grade 2 treatment effect was associated with a PPV and NPV of 0.91 and 0.89, while grade 3 or greater treatment effect had PPV and NPV of 1.00 and 0.45 for development of subsequent urethral fragmentation. Achieving grade 3 damage on POD 0 endoscopy was associated with the development of gross urethral disintegration within 24 hours on follow-up endoscopy in 8/9 (88.9%) subjects.

In three subjects with very small prostates (mean 19.9 cc), rectoprostatic fistulae occurred but were managed conservatively. Urinary retention developed in one additional subject on POD 2 that was managed with an indwelling urinary catheter for 48 hours; the subject subsequently did well.

Discussion

In the present study, we characterized the dose-dependent endoscopic appearance and chronologic progression of

Table 1. Endoscopic Assessment of Urethral Treatment Effect as a Predictor of the Development of Urethral Disintegration by Postoperative Day 14

Visualized treatment effect	*Sensitivity*	*Specificity*	*PPV*	*NPV*	*Accuracy*
≥Grade 1	1.00	0.30	0.75	1.00	0.77
≥Grade 2	0.95	0.80	0.91	0.89	0.90
≥Grade 3	0.38	1.00	1.00	0.45	0.58

PPV = photoselective vaporization of the prostate; NPV = negative predictive value.

histotripsy treatment effect from normal urethra to disintegration of the prostatic urethra. We then used these findings to develop a grading scale to characterize the endoscopic appearance of the urethral treatment effect. While only 8.6% of histotripsy treatments resulted in acute urethral disintegration, nearly 70% of treated zones ultimately exhibited urethral disintegration within 2 weeks of treatment, indicating that acute urethral fragmentation is not a reliable measure of urethral damage. Such observations indicate an opportunity to optimize effective treatment of the prostatic urethra to ensure adequate tissue debulking and creation of a TURP-like defect.

Although histotripsy allows for noninvasive transcutaneous treatment of the canine prostate,[12–14] this study specifically assessed the utility of postprocedure endoscopy as a strategy to guide treatment of the prostatic urethra. The finding of urothelial shedding (grade 2) on immediate postprocedure cystoscopy was associated with a greater than 90% success rate (PPV 0.91) of development of urethral disintegration within 2 weeks of treatment. Further, producing a flap of urothelium (grade 3) postprocedure was associated with the development of frank urethral disintegration within 24 hrs of the procedure in nearly 90% of cases. Such findings indicate that cystoscopy could play a role in treating to a desired amount of acute urethral damage to achieve subacute or chronic urethral disintegration.

The observation of debris within treatment cavities adjacent to intact urethra suggests that urethral disintegration may be needed for rapid drainage of homogenized adenoma and effective tissue debulking for creation of a TURP-like defect. The significance of undrained cavities remains to be determined, however, including the chronicity of their evolution and if cavity drainage is necessary for prostate histotripsy treatment success.

While direct tissue fractionation from cavitation is clearly of importance to the mechanism of action of histotripsy,[8–10] our data imply that there may be additional treatment effects that contribute to the development of urethral disintegration. Specifically, the observation that urethral disintegration develops in 66% (21/32) of treatment zones chronically within 2 weeks in subjects without acute evidence of disintegration has led us to hypothesize that there may be a component of tissue ischemia contributing to urethral disintegration. This hypothesis is supported by the observed progression of treatment effect from the formation of petechial hemorrhage and active bleeding to relative hemostasis and the appearance of pale, gray, shaggy urothelium.

Initially, histotripsy damage may disrupt capillaries and small vessels, leading to bleeding and hemorrhage. As damage increases, vascular structures may be completely destroyed, causing hemostasis, while other urethral structures begin to show damage, such as shedding of the urothelium. Resulting ischemia leads to breakdown and disintegration of the partially fragmented portions of the urethra in the periprocedure period, allowing drainage of the periurethral cavity. Such a progression, could potentially account for the improved positive predictive value of grade 2 damage (pale, potentially ischemic urothelium) compared with grade 1 damage (potentially viable, bleeding urothelium) at predicting the evolution of urethral disintegration in the chronic setting. Finally, a role for capillary/vascular damage in the effectiveness of prostate histotripsy would also provide an explanation for the reason prostate histotripsy is associated with minimal hematuria, even in the setting of anticoagulation.[14] Further studies are ongoing to address this hypothesis.

Optimal prostate histotripsy treatment strategy remains to be determined, and the generalizability of these results from canine to human prostate is uncertain. Structurally, the canine prostate is bilobed without zonal structures, whereas the human prostate is subdivided into several different zones, with potentially different treatment thresholds, with the transition zone being most relevant to BPH. The vascular anatomy of the prostate, however, is very similar between the two species, with arterial branches from the internal pudendal artery perforating the capsule to supply the stroma and glandular tissues with the venous drainage in close proximity.[15] In addition, the intraperitoneal location of the canine prostate lends itself to a transabdominal histotripsy approach, whereas structural modeling suggests that the human prostate will likely be more amenable to a transperineal approach[16] or transrectal approach. Ultimately, human studies are needed to determine both the clinical efficacy and optimal treatment algorithm for prostate histotripsy.

Conclusion

In a canine model, prostate histotripsy targeting the urethra results first in hemorrhage, followed by hemostasis and shedding of the urothelium, subsequent urothelial flap creation, and finally urethral disintegration. Acute urethral fragmentation after histotripsy of the prostate is not necessary to achieve urethral disintegration in the chronic setting, however. Treating until endoscopic evidence of urothelial shedding is present (grade 2 treatment effect) may be a strategy (PPV 0.91) to achieve reliable urethral disintegration. Further studies are needed to determine if urethral disintegration is necessary for maximal treatment benefit and how reliably these findings transfer to the human prostate.

Acknowledgments

We would like to thank Kim Ives, D.V.M., for her outstanding and dedicated veterinary care, without which this study would not have been possible.

Funding provided by NIH grant RO1DK087871.

Disclosure Statement

Drs. Roberts and Hall have equity, royalty, and consulting interests in HistoSonics, Inc. For the remaining authors, No competing financial interests exist.

References

1. Ahyai SA, Lehrich K, Kuntz RM. Holmium laser enucleation versus transurethral resection of the prostate: 3-year follow-up results of a randomized clinical trial. Eur Urol 2007;52: 1456–1463.
2. Ruszat R, Seitz M, Wyler SF, et al. GreenLight laser vaporization of the prostate: Single-center experience and long-term results after 500 procedures. Eur Urol 2008;54:893–901.
3. Larson TR. Current treatment options for benign prostatic hyperplasia and their impact on sexual function. Urology 2003;61:692–698.
4. McVary KT, Roehrborn CG, Avins AL, et al. Guideline on the Managment of Benign Prostatic Hyperplasia (BPH). 2010. Available at: http://www.auanet.org/content/guidelines-

and-quality-care/clinical-guidelines.cfm?sub=bph. Accessed April 5, 2011.
5. McVary KT, Roehrborn CG, Avins AL, et al. Update on AUA guideline on the management of benign prostatic hyperplasia. J Urol 2011;185:1793–1803.
6. Wei JT, Calhoun E, Jacobsen SJ. Urologic diseases in America project: Benign prostatic hyperplasia. J Urol 2005; 173:1256–1261.
7. Lake AM, Hall TL, Kieran K, et al. Histotripsy: Minimally invasive technology for prostatic tissue ablation in an in vivo canine model. Urology 2008;72:682–686.
8. Xu Z, Raghavan M, Hall TL, et al. High speed imaging of bubble clouds generated in pulsed ultrasound cavitational therapy—histotripsy. IEEE Trans Ultrason Ferroelectr Freq Control 2007;54:2091–2101.
9. Xu Z, Fowlkes JB, Rothman ED, et al. Controlled ultrasound tissue erosion: The role of dynamic interaction between insonation and microbubble activity. J Acoust Soc Am 2005; 117:424–435.
10. Tran BC, Seo J, Hall TL, et al. Microbubble-enhanced cavitation for noninvasive ultrasound surgery. IEEE Trans Ultrason Ferroelectr Freq Control 2003;50:1296–1304.
11. Kieran K, Hall TL, Parsons JE, et al. Refining histotripsy: Defining the parameter space for the creation of nonthermal lesions with high intensity, pulsed focused ultrasound of the in vitro kidney. J Urol 2007;178:672–676.
12. Hempel CR, Hall TL, Cain CA, et al. Histotripsy fractionation of prostate tissue: Local effects and systemic response in a canine model. J Urol 2011;185:1484–1489.
13. Hall TC, Hempel CR, Wojno K, et al. Histotripsy of the prostate: dose effects in a chronic canine model. Urology 2009;74:932–937.
14. Wheat JC, Hall TL, Hempel CR, et al. Prostate histotripsy in an anticoagulated model. Urology 2010;75:207–211.
15. Evans HE. Miller's Anatomy of the Dog. Philadelphia, PA: WB Saunders, 1993, 514–516.
16. Hall TL, Hempel CR, Sabb BJ, et al. Acoustic access to the prostate for extracorporeal ultrasound ablation. J Endourol 2010;24:1875–1881.

Address correspondence to:
William W. Roberts, M.D.
Department of Urology
University of Michigan TC 3879
1500 E. Medical Center Drive
Ann Arbor, MI 48109

E-mail: willrobe@med.umich.edu

Abbreviations Used

BPH = benign prostatic hyperplasia
NPV = negative predictive value
POD = postoperative day
PPV = positive predictive value
TRUS = transrectal ultrasound
TURP = transurethral resection of the prostate
US = ultrasound

This article has been cited by:

1. George R. Schade, Timothy L. Hall, William W. Roberts. 2012. Urethral-sparing Histotripsy of the Prostate in a Canine Model. *Urology* **80**:3, 730-735. [CrossRef]